

# Vertical-Cavity Surface-Emitting Lasers With Monolithically Integrated Horizontal Waveguides

H. C. Lin, *Member, IEEE*, D. A. Louderback, *Member, IEEE*, G. W. Pickrell, *Member, IEEE*,  
M. A. Fish, *Member, IEEE*, J. J. Hindi, M. C. Simpson, and P. S. Guilfoyle, *Senior Member, IEEE*

**Abstract**—We present the development of novel 980-nm  $\text{Ga}_{0.8}\text{In}_{0.2}\text{As}$ -GaAs vertical-cavity surface-emitting lasers (VCSELs) with an internal waveguide structure. The monolithic integration of a horizontal waveguide in the top distributed Bragg reflector (DBR) creates the potential for achieving VCSEL-based photonic integrated circuits. In this work, an AlGaAs-GaAs-AlGaAs waveguide designed for horizontal propagation of light was monolithically integrated as part of the upper GaAs-AlGaAs DBR of the device. VCSELs with 9- $\mu\text{m}$  apertures emitted 3-mW single-mode power with both longitudinal and lateral mode suppression ratio of 40 dB under room-temperature continuous-wave operation.

**Index Terms**—Monolithic integration, single mode, vertical-cavity surface-emitting laser (VCSEL), waveguide.

## I. INTRODUCTION

VERTICAL-CAVITY surface-emitting lasers (VCSELs) have a great potential for monolithic integration with other components such as detectors, modulators, gratings, and waveguides to form photonic integrated circuits on a single platform [1]–[3]. To enable data communication between the VCSEL and the other components on the same substrate, we have designed and fabricated 980-nm  $\text{Ga}_{0.8}\text{In}_{0.2}\text{As}$ -GaAs VCSELs with an internal waveguide structure located in the upper GaAs-AlGaAs distributed Bragg reflector (DBR). The monolithic AlGaAs-GaAs-AlGaAs waveguide was designed for wave propagation in the horizontal direction, in plane with the substrate. The light oscillating inside the VCSEL cavity can be coupled into the horizontal waveguide by means of diffraction gratings for bidirectional data communications, power monitoring, built-in test, and wavelength-division multiplexing [4], [5]. In this letter, the 980-nm VCSEL with an internal waveguide was demonstrated without diffraction gratings, as the primary step toward the monolithic integration of multiple components. The integration scheme effectively suppressed the sidemodes in large-aperture devices yielding a higher possible single-mode output power. To the best of our knowledge, this demonstration represents the first monolithically integrated device structure combining VCSELs and waveguides.

Manuscript received June 1, 2004; revised August 16, 2004. This work was supported in part by the Missile Defense Agency (MDA), in part by the Naval Air Systems Command (NAVAIR), and in part by the Air Force Research Laboratory (AFRL).

The authors are with OptiComp Corporation, Zephyr Cove, NV 89448 USA (e-mail: hclin@opticomp.com).

Digital Object Identifier 10.1109/LPT.2004.837483

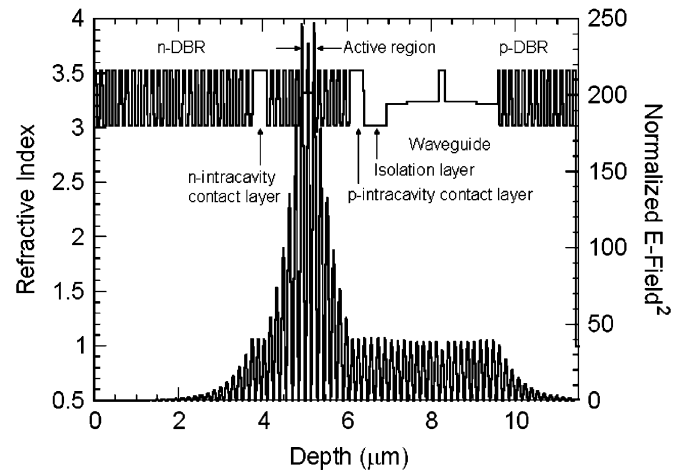


Fig. 1. Refractive index and optical standing wave profile modeled for a 980-nm VCSEL with an internal waveguide placed in the seventh period of the top DBR. From left to right, the profile corresponds to the device structure from the substrate to the top. The peak of the optical power envelope overlaps the QWs centered in the  $1 - \lambda$  VCSEL cavity.

## II. DESIGN OF VCSEL WITH AN INTERNAL WAVEGUIDE

The integrated VCSEL-waveguide structure was modeled using internally developed software based on the transfer matrix method. The index and optical standing wave profiles for the modeled VCSEL with an internal waveguide are shown in Fig. 1. From the left (bottom) of the profile, the device employs a 30.5-period  $\text{Al}_{0.87}\text{Ga}_{0.13}\text{As}$ -GaAs n-type lower DBR for providing a reflectivity of 99.995%, not including any loss mechanisms. An n-type GaAs intracavity contact layer of 335 nm is inserted inside the n-DBR in the sixth DBR period from the active region. The  $1 - \lambda$   $\text{Al}_{0.3}\text{Ga}_{0.7}\text{As}$ -GaAs VCSEL cavity contains three 8-nm  $\text{Ga}_{0.8}\text{In}_{0.2}\text{As}$  quantum wells (QWs) separated by 8-nm GaAs barriers within the  $\text{Al}_{0.3}\text{Ga}_{0.7}\text{As}$  separate confinement heterostructure layers. The peak of the optical standing wave is centered within the central cavity of the structure, where the gain media is located. To the right (top) of the cavity is the 19-period  $\text{Al}_{0.87}\text{Ga}_{0.13}\text{As}$ -GaAs p-type upper DBR. A 40-nm  $\text{Al}_{0.98}\text{Ga}_{0.02}\text{As}$  aperture layer was included in the first period of the p-type DBR. A p-type GaAs intracavity contact layer is included in the sixth period of the upper DBR and is followed by a 520-nm  $\text{Al}_{0.87}\text{Ga}_{0.13}\text{As}$  isolation layer. The isolation layer is used to isolate the waveguide from the GaAs intracavity contact layer, which has a higher refractive index and a higher doping concentration. Above the AlGaAs isolation layer are the layers that comprise the waveguide, including a 200-nm GaAs core, a pair of 750-nm  $\text{Al}_{0.46}\text{Ga}_{0.54}\text{As}$

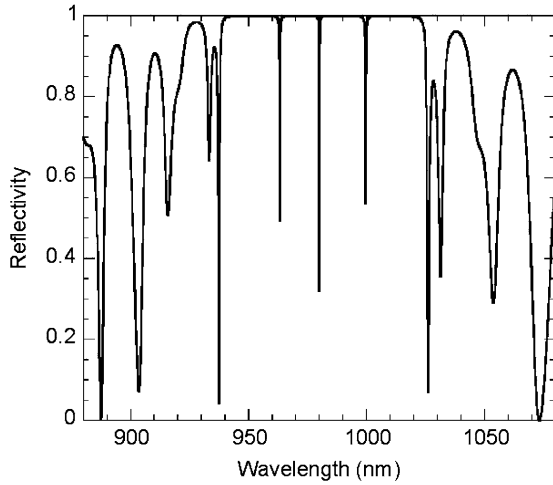


Fig. 2. Simulated reflectivity spectrum for a 980-nm VCSEL with an internal waveguide placed in the seventh period of the top DBR. Three resonances appear in the stopband at 963, 980, and 999 nm, respectively, due to the existence of the waveguide layer inside the VCSEL.

inner claddings, and a pair of 500-nm  $\text{Al}_{0.5}\text{Ga}_{0.5}\text{As}$  outer cladding layers. The waveguide was designed to exhibit a mode size similar to that of a tapered optical fiber. The waveguide was placed in the seventh period of the top DBR, where the waveguide and the isolation layer function both as a waveguide and a DBR period. This is achieved by choosing the appropriate index profiles and layer thicknesses for the waveguide, as well as a total thickness that maintains correct vertical phasing in the DBR.

Fig. 2 shows the modeled reflectivity spectrum for this structure, showing the DBR stopband, as well as several minima in the reflectivity due to cavity resonances. Within the stopband, three cavity modes are located at approximately 963, 980, and 999 nm. In a typical VCSEL structure, there is only one cavity mode located at the desired lasing wavelength. Including the waveguide in the VCSEL structure leads to the appearance of several more modes in addition to the central cavity mode at 980 nm. Since a relatively small growth deviation could cause the waveguide to become a multiple of  $\lambda/2$  in thickness and behave as a resonant cavity, precautions have been taken to ensure that the structure will only lase in the designed cavity mode and not in the other modes introduced by the waveguide. First of all, since the waveguide is located in the top DBR, the transmission losses, if the waveguide acted as a cavity, are higher than that of the central cavity. Therefore, the modes introduced by the waveguide will be too lossy to achieve lasing threshold even if the gain peak of the QWs shifts. Second, those sidemodes should receive less optical gain from the  $\text{Ga}_{0.8}\text{In}_{0.2}\text{As}$ -GaAs QWs designed for an optical emission at 980 nm. The results of our modeling efforts were verified with experimental demonstration of the integrated VCSEL-waveguide structure.

### III. EPITAXIAL GROWTH AND DEVICE FABRICATION

The designed structure was grown using a Veeco Applied Epi Gen III molecular beam epitaxy system on an n-type 3" GaAs wafer. After an n-doped GaAs buffer layer, the n-type  $\text{Al}_{0.87}\text{Ga}_{0.13}\text{As}$ -GaAs DBR was grown at a substrate

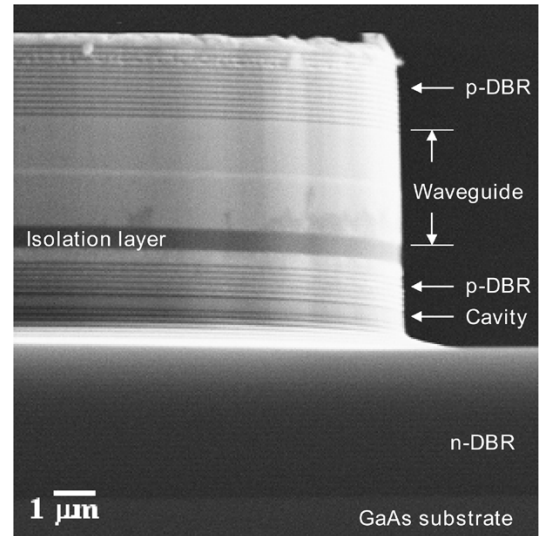


Fig. 3. SEM micrograph of the cross section for a fabricated VCSEL with an internal waveguide.

temperature of 580 °C measured using an infrared pyrometer at a growth rate of approximately 1.5 monolayers per second. The As-overpressure used for the growth of the DBRs was about  $1 \times 10^{-6}$  Torr, as measured by an ion gauge. The n-type DBR was doped with Si to a concentration of  $3 \times 10^{18} \text{ cm}^{-3}$ . The growth temperature was reduced to 560 °C for the growth of the QW active region and the As-overpressure was increased to  $3 \times 10^{-6}$  Torr. During the growth of the top DBR, the growth temperature and As-overpressure were returned to their original values. A gaseous source,  $\text{CBr}_4$ , was used to supply carbon, a p-type dopant, to a concentration of  $4 \times 10^{18} \text{ cm}^{-3}$  for the p-type DBR. Both the n- and p-type doping concentrations in the DBRs were decreased to levels around  $1 \times 10^{18} \text{ cm}^{-3}$  at vicinity of the active region. To reduce the electric resistance of the DBR, linear and uniparabolic compositional grading schemes were used in growing the AlGaAs layers for the n- and p-type DBRs, respectively [6].

The wafer was then removed from the growth chamber for device fabrication. Photolithography was employed to pattern the top ring contact. Then, Ti-Pt-Au and Ni-Au-Ge-Ni-Au were deposited using e-beam evaporation for the p- and n-contacts, respectively. After the metallization,  $\text{Cl}_2$  reactive ion etching (RIE) was used to create the VCSEL mesas. The etch depth was chosen to allow exposure of the aperture layer for lateral oxidation. After the RIE process, the sample was placed in a single-zone quartz furnace for wet oxidation of the current aperture. During the oxidation process, the metal contacts were alloyed at the same time to finish the fabrication process.

### IV. RESULTS AND DISCUSSIONS

Fig. 3 is the cross-sectional scanning electron microscopy (SEM) micrograph of the fabricated device depicting the layer structure of the VCSEL-waveguide integration. As seen in the figure, the device demonstrated a vertical mesa profile with a smooth sidewall and a shallow shoeing after the fabrication process. The continuous-wave (CW) operating behavior of the

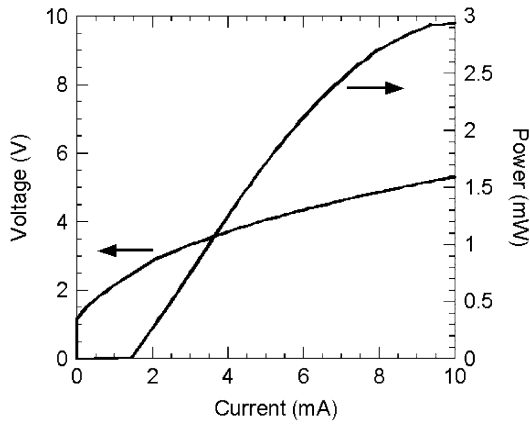


Fig. 4.  $L$ - $I$ - $V$  characteristics of a  $9\text{-}\mu\text{m}$  aperture VCSEL with a monolithically integrated waveguide in the seventh period of the top DBR. The device was measured under RT CW operations.

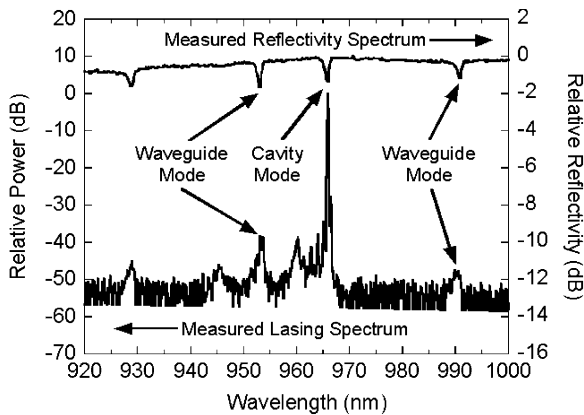


Fig. 5. Measured reflectivity and lasing spectra for a  $9\text{-}\mu\text{m}$  aperture VCSEL with an internal waveguide. As the spectra indicate, the VCSEL lases single mode, both longitudinally and laterally, in the desired cavity mode.

VCSEL with an internal waveguide was measured at room temperature (RT). Fig. 4 shows the light-current-voltage ( $L$ - $I$ - $V$ ) characteristics for a device with an aperture size of  $9\text{ }\mu\text{m}$  in diameter. The device has a low threshold current of 1.4 mA and a peak output power of 3 mW.

The spectrum of the device was analyzed using an optical spectrum analyzer. Fig. 5 shows the lasing spectra of a  $9\text{-}\mu\text{m}$  VCSEL with an internal waveguide in parallel with the measured reflectivity spectrum of the as-grown VCSEL structure. The VCSEL-waveguide operates single mode both longitudinally and laterally as it was designed. The waveguide modes on either side of the cavity mode are not lasing and their powers are each at least 40 dB lower than the desired lasing mode of the main cavity. In addition, as the spectrum shows, the VCSEL-waveguide combination lases in a single lateral mode with approximately 40-dB sidemode suppression ratio (SMSR). Typical VCSELs with the same aperture size would be multimode laterally, but the unusually long effective cavity length of these devices caused them to lase in a single lateral mode. Other researchers have noticed similar effects for extended cavity VCSELs, where the long cavity length introduced larger diffraction losses for the higher order modes

[7]. Nevertheless, the long effective cavity length reported in this letter is a result of the additional waveguide structure located in the top mirror, instead of an extended cavity with unwanted additional longitudinal modes that could lase. The measured single longitudinal and lateral mode result supports the modeling effort for the integrated VCSEL-waveguide structure. This property also enables these devices to exhibit a high single-mode power that is advantageous to many applications.

## V. CONCLUSION

$\text{Ga}_{0.8}\text{In}_{0.2}\text{As}$ -GaAs VCSELs at 980 nm with a monolithically integrated waveguide structure have been demonstrated. The waveguide is in plane with the wafer surface to facilitate horizontal communication, enabling VCSEL-based photonic integrated circuits in future designs. The modal properties of the integrated VCSEL-waveguide structure were investigated, both theoretically and experimentally, for efficient single-mode operations. The output power measured from a  $9\text{-}\mu\text{m}$  aperture VCSEL is 3 mW, and the threshold current is 1.4 mA under RT CW conditions. In addition, a single longitudinal and lateral mode with an SMSR of larger than 40 dB was observed from the same device. The long effective cavity contributed to single longitudinal and lateral mode operation and the 40-dB SMSR. The modal behavior of the fabricated VCSEL is consistent with the measured cavity reflectivity. The power performance of the device can be enhanced by adopting intracavity contacts for an undoped waveguide in the future development. We believe that the monolithic integration of VCSELs and waveguides, as accomplished in this work, will be useful in many new optoelectronic applications.

## REFERENCES

- [1] J. S. Barton, E. J. Skogen, M. L. Masanovic, S. P. Denbaars, and L. A. Coldren, "A widely-tunable high-speed transmitter using an integrated SGDBR laser-semiconductor optical amplifier and Mach-Zehnder modulator," *IEEE J. Sel. Topics Quantum Electron.*, vol. 9, no. 5, pp. 1113-1117, Sep./Oct. 2003.
- [2] S. F. Lim, J. A. Hudgings, L. P. Chen, G. S. Li, W. Yuen, K. Y. Lau, and C. J. Chang-Hasnain, "Modulation of a vertical-cavity surface-emitting laser using an intracavity quantum-well absorber," *IEEE Photon. Technol. Lett.*, vol. 10, no. 3, pp. 319-321, Mar. 1998.
- [3] O. Sjolund, D. A. Loderback, E. R. Hegblom, J. Ko, and L. A. Coldren, "Monolithic integration of substrate input/output resonant photodetectors and vertical cavity lasers," *IEEE J. Quantum Electron.*, vol. 35, no. 7, pp. 1015-1023, Jul. 1999.
- [4] G. W. Pickrell, C. F. Xu, D. A. Loderback, H. C. Lin, M. A. Fish, J. J. Hindi, M. C. Simpson, P. S. Guilfoyle, Z. H. Zhang, and K. C. Hsieh, "Molecular beam epitaxial regrowth on diffraction gratings for VCSEL-based integrated optoelectronics," *J. Appl. Phys.*, vol. 96, no. 8, pp. 4050-4055, Oct. 2004.
- [5] D. A. Loderback, G. W. Pickrell, H. C. Lin, M. A. Fish, J. J. Hindi, and P. S. Guilfoyle, "VCSELs with monolithic coupling to internal horizontal waveguides using integrated diffraction gratings," *Electron. Lett.*, vol. 40, no. 17, pp. 1064-1065, Aug. 2004.
- [6] G. W. Pickrell, D. A. Loderback, M. A. Fish, J. J. Hindi, H. C. Lin, M. C. Simpson, P. S. Guilfoyle, and K. L. Lear, "Compositional grating in distributed Bragg reflectors using discrete alloys in vertical-cavity surface emitting lasers," *J. Cryst. Growth*, submitted for publication.
- [7] H. J. Unold, S. W. Z. Mahmoud, R. Jäger, M. Kicherer, M. C. Riedl, and K. J. Ebeling, "Improving single-mode VCSEL performance by introducing a long monolithic cavity," *IEEE Photon. Technol. Lett.*, vol. 12, no. 8, pp. 939-941, Aug. 2000.